
Upper Limits of Diffuse Gamma Rays from the Galactic Plane at 10 TeV with the Tibet II and III Arrays

(The Tibet AS γ Collaboration)

M. Amenomori and H. Nanjo

Department of Physics, Hirosaki University, Hirosaki 036-8561, Japan

S. Ayabe and K. Mizutani

Department of Physics, Saitama University, Saitama 338-8570, Japan

S.H. Cui, L.K. Ding, H.B. Hu, C.L. Lan, H. Lu, S.L. Lu, J.R. Ren, Y.H. Tan, B.S. Wang, H. Wang, H.M. Zhang and J.L. Zhang

Laboratory of Cosmic Ray and High Energy Astrophysics, Institute of High Energy Physics, Chinese Academy of Sciences, Beijing 100039, China

Danzengloubu, X.H. Ding, H.W. Guo, Labaciren, X.R. Meng, A.F. Yuan and Zhaxisangzhu

Department of Mathematics and Physics, Tibet University, Lhasa 850000, China

C.F. Feng, M. He, J.Y. Li, Y.G. Wang, L. Xue, N.J. Zhang and X.Y. Zhang

Department of Physics, Shandong University, Jinan 250100, China

Z.Y. Feng, Q. Huang, H.Y. Jia, G.C. Yu and X.X. Zhou

Institute of Modern Physics, South West Jiaotong University, Chengdu 610031, China

X.Y. Gao, Q.X. Geng, J. Mu and X.C. Yang

Department of Physics, Yunnan University, Kunming 650091, China

K. Hibino, T. Sasaki, T. Shirai, N. Tateyama, S. Torii and T. Utsugi

Faculty of Engineering, Kanagawa University, Yokohama 221-8686, Japan

N. Hotta, J. Huang, I. Ohta and S. Ozawa

Faculty of Education, Utsunomiya University, Utsunomiya 321-8505, Japan

M. Izumi, F. Kajino, K. Kawata, M. Sakata and Y. Yamamoto

Department of Physics, Konan University, Kobe 658-8501, Japan

K. Kasahara

Faculty of Systems Engineering, Shibaura Institute of Technology, Saitama 330-8570, Japan

Y. Katayose and M. Shibata

Faculty of Engineering, Yokohama National University, Yokohama 240-0067, Japan

G.M. Le and Z.H. Ye

Center of Space Science and Application Research, Chinese Academy of Sciences, Beijing 100080, China

M. Nishizawa

National Institute for Informatics, Tokyo 112-8640, Japan

M. Ohnishi, T. Ouchi, A. Shiomi, M. Takita and H. Tsuchiya

Institute for Cosmic Ray Research, University of Tokyo, Kashiwa 277-8582, Japan

T. Saito

Tokyo Metropolitan College of Aeronautical Engineering, Tokyo 116-0003, Japan

H. Sugimoto and K. Taira

Shonan Institute of Technology, Fujisawa 251-8511, Japan

T. Yuda

Solar-Terrestrial Environment Laboratory, Nagoya University, Nagoya 464-8601, Japan

Abstract

Diffuse gamma rays from the Galactic plane were searched combining the Tibet II and III data at 10 TeV region. The number of used events are increased by 1.6 times than the previous analysis with the Tibet II. The sky regions searched are the inner Galaxy, $20^\circ \leq l \leq 55^\circ$, and outer Galaxy, $140^\circ \leq l \leq 225^\circ$ with the plane thickness $|b| \leq 2^\circ$. Although no significant excess was observed, the intensity upper limits with 99% confidence level at 10 TeV are reduced by factors of 0.70 and 0.82 than the previous ones, respectively, assuming a differential spectral index of 2.4. The present results give the most stringent upper limits on the inverse Compton model with a source electron spectral index of 2.0.

EGRET observations (Hunter et al. 1997) gave a detailed intensity distribution of high-energy gamma rays coming from the Galactic plane. The gamma-ray intensity above 1 GeV from the inner Galaxy is higher than the COS B data by a factor of about 3. It is also higher than the conventional model predictions (e.g., Bertsch et al. 1993) by a factor of 1.7, assuming the power law source proton spectrum with an index of 2.75. Mori (1997) showed that the EGRET excess can be interpreted by adopting a harder proton spectral index of 2.45 within a plane thickness of $|b| \leq 10^\circ$. Webber (1999) also showed that the excess in $|b| \leq 5^\circ$ can be reproduced by a source proton spectral index of 2.25.

Porter & Protheroe (1997) indicated that in such a high-energy region, cosmic-ray electrons may create a significant part of the diffuse gamma rays. Pohl & Esposito (1998) argued that if the injection electron index of 2.0 is employed, the EGRET excess above 1 GeV can be well explained by the inverse Compton (IC) scattering. At the TeV-PeV region, the diffuse gamma-ray emission was calculated by Berezhinsky et al. (1993) in terms of cosmic-ray interaction with the interstellar matter (ISM).

In the previous paper (Amenomori et al. 2002) we analyzed the Tibet II data at 10 TeV and the Tibet III data at 3 TeV. In this paper we report new upper limits combining the Tibet II and III data at 10 TeV.

The Tibet II array with 221 scintillation counters of 0.5 m^2 each, was constructed at Yangbajing (4300 m a.s.l.) in 1994, keeping the same lattice interval of 15 m as the Tibet I. The performance of the Tibet II is almost same as the Tibet I (Amenomori et al. 1992, 1993). The mode energy is 10 TeV for air showers with $\Sigma_{\rho_{\text{FT}}} \geq 15 \text{ m}^{-2}$, where $\Sigma_{\rho_{\text{FT}}}/2$ is the sum of the number of particles that hit all 0.5 m^2 detectors. The angular resolution is about 0.9° at 10 TeV, calibrated by

using the deficit shape of the Moon shadow (Amenomori et al. 1993, 1996). The Tibet III array, enlarged in 1999, consists of 533 counters with a 7.5 m lattice interval. The additional detectors are excluded in the present analysis so as to keep a same performance as the Tibet II.

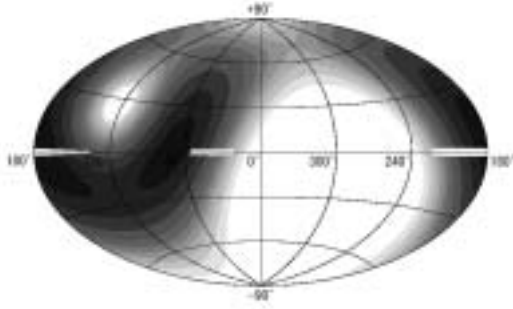


Fig. 1. Exposure map for the Tibet III.

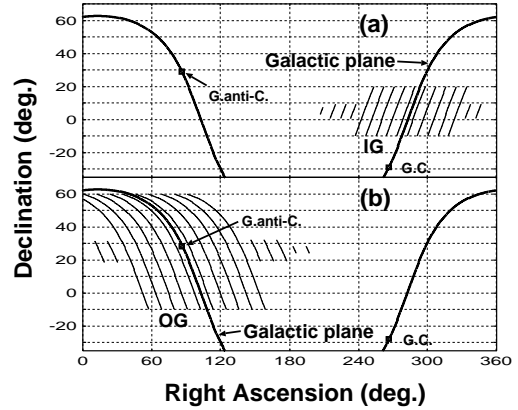


Fig. 2. Binning of warped belts.

Figure 1 shows an exposure map in the galactic coordinates for air showers obtained with the Tibet III array, for example, with zenith angles $\theta \leq 50^\circ$. The shower event density increases from light gray to dark gray. For the on-plane data, shower events are employed in the sky regions of $20^\circ \leq l \leq 55^\circ$ for the inner Galaxy (IG) and of $140^\circ \leq l \leq 225^\circ$ for the outer Galaxy (OG), both in $|b| \leq 2^\circ$ along the Galactic plane.

The experimental data are analyzed in the basically same manner as the previous paper (Amenomori et al. 2002), except for binning width of warped belts in the right ascension. In the present case, air shower events are assigned to the sky regions from which they arrived, of 4.5° (5.625°) bin 80 (64) belts along the Galactic plane of the inner (outer) Galaxy in the equatorial coordinates both for the Tibet II and III data, as shown in Fig. 2, which shows 4.5° bin warped belts for (a) IG with the declination range of $-10^\circ \leq \delta \leq 20^\circ$ and 5.625° bin belts for (b) OG with $-10^\circ \leq \delta \leq 60^\circ$. These declination ranges of the on-plane belts in the equatorial coordinates correspond to parts of thin convex lens shape zones, shown in Fig. 1, with an average thickness of 4° in the galactic coordinates.

One reason those warped belts are used is to detect gamma-ray signals as accurately as possible if the Galactic plane gamma-ray intensity is greater than the isotropic component. In addition, the zenith angle distribution, and hence the primary energies of detected air showers are quite similar in each warped belt. So the on-plane background estimation can be done at the same energy as many

off-plane belts. Finally, the background estimate, especially for the OG, is little affected by the IG plane, because the warped belts crossing the IG plane do so diagonally, over a narrow band of longitudes.

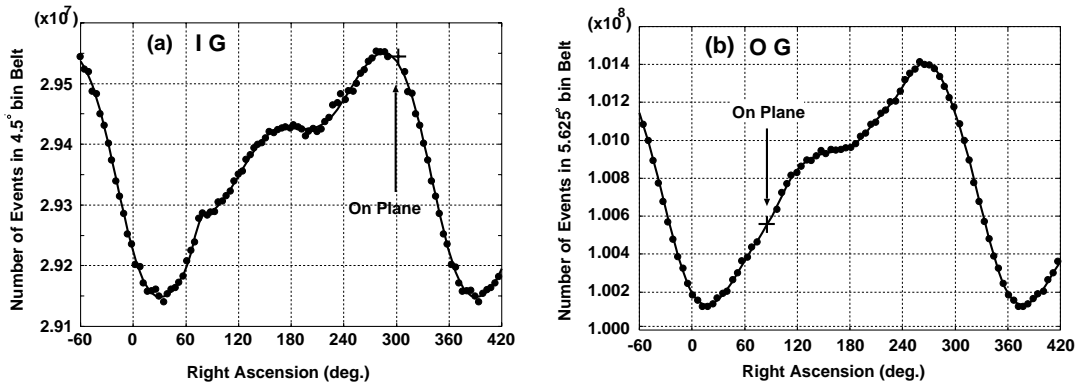


Fig. 3. Right ascension distribution of number of events for (a) IG and (b) OG.

Figure 3 shows the distribution of the number of events in (a) 4.5° and (b) 5.625° bin warped belts for IG and OG, respectively. The abscissa represents the right ascension of each warped belt at the declination 30° , which is the same as the latitude of the Yangbajing site. The solid lines are the curves fitted to the experimental data, ignoring the on-plane data. The anisotropy of cosmic-ray intensity seen in this figure, with an amplitude within $\pm 1\%$, is mainly due to some seasonal suspensions of operation for construction and system calibration.

An excess of the on-plane data over the fitted curve is measured by a standard deviation of the number of showers by the formula $(E - B)/\sqrt{B}$, in two 2.25° (IG) or three 1.875° (OG) bin belts, where E is the number of on-plane events and B is the estimated number of background events in the on-plane region. B is estimated from the solid curve which is obtained by fitting of many off-plane belts, ignoring both the central 13.5° width in right ascension ($|b| \leq 6^\circ$) for IG and 20.625° ($-7.3^\circ \leq b \leq 6.0^\circ$) for OG. The solid curves in Figure 3, (a) for IG and (b) for OG, indicate the number of the galactic cosmic rays.

The deviation distributions of the number of off-plane events from the fitted solid curves are represented by best-fit Gaussians with standard deviations of 1.002 and 0.998 for IG and OG planes, respectively. Each standard deviation is almost equal in unity, so the solid curves are considered to be satisfactorily fitted to the experimental data. Thus, we can accurately estimate the number of on-plane background events.

The significance of an on-plane excess is given in Table 1. No significant excess is found. We calculate the gamma-ray flux ratio, J_γ/J_{CR} , for 90% CL

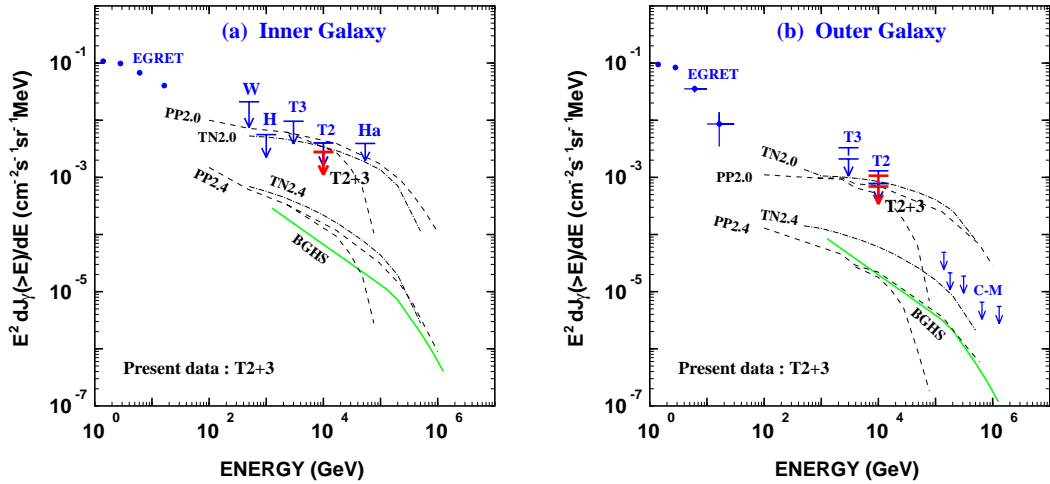


Fig. 4. Diffuse gamma rays from the Galactic planes for (a) IG and (b) OG.

and 99% CL upper limits, to the galactic cosmic rays at 10 TeV. The differential intensity multiplied by E^2 with these upper limits are also given for IG and OG, assuming gamma-ray spectral index of 2.4. Thus, we can calculate the intensity upper limits in 99% CL, as $2.8 \times 10^{-17} \text{ cm}^{-2} \text{ s}^{-1} \text{ MeV}^{-1}$ for IG and $1.07 \times 10^{-17} \text{ cm}^{-2} \text{ s}^{-1} \text{ MeV}^{-1}$ for OG with $|b| \leq 2^\circ$ at 10 TeV, using the all-particle energy spectrum of the galactic cosmic rays compiled by Apanasenko et al. (2001).

Table 1

Inner or Outer Galactic Plane (Regions of l, b)	Significance (σ)	$1/\sqrt{B}$ at 10 TeV (10^{-4})	$\frac{J_\gamma(>E)}{J_{\text{CR}}(>E)}$ at 10 TeV 90% CL (10^{-4})	$\frac{J_\gamma(>E)}{J_{\text{CR}}(>E)}$ at 10 TeV 99% CL (10^{-4})	$E^2 \frac{dJ_\gamma(>E)}{dE}$ (cm $^{-2}$ s $^{-1}$ sr $^{-1}$ MeV) 90% CL (10^{-3})	$E^2 \frac{dJ_\gamma(>E)}{dE}$ (cm $^{-2}$ s $^{-1}$ sr $^{-1}$ MeV) 99% CL (10^{-3})
I G ($20^\circ \leq l \leq 55^\circ$) ($-2^\circ \leq b \leq 2^\circ$)	+1.27	1.84	4.81	6.71	2.0	2.8
O G ($140^\circ \leq l \leq 225^\circ$) ($-2^\circ \leq b \leq 2^\circ$)	+0.05	0.997	1.68	2.60	0.69	1.07

Figure 4 shows the 99% CL upper limits (T2+3) thus obtained for diffuse gamma rays from (a) IG, $20^\circ \leq l \leq 55^\circ$ and (b) OG, $140^\circ \leq l \leq 225^\circ$ both with $|b| \leq 2^\circ$, at 10 TeV. In this figure the Tibet upper limits with 99% CL are plotted for the Tibet II (T2) at 10 TeV and for the Tibet III (T3) at 3 TeV (Amenomori et al. 2002). The EGRET data (Hunter et al. 1997) are plotted for (a) IG in $315^\circ \leq l \leq 45^\circ$ and (b) OG in $135^\circ \leq l \leq 225^\circ$, both with $|b| \leq 2^\circ$. In subfigure (a) are plotted the Cerenkov data including Whipple’s 99.9% CL upper limit above 500 GeV (LeBohec et al. 2000) at the region of $38.5^\circ \leq l \leq 41.5^\circ$

with $|b| \leq 2^\circ$, and HEGRA-IACT's 99% CL upper limit above 1 TeV (Aharonian et al. 2001) in a similar region of $38^\circ \leq l \leq 43^\circ$ with $|b| \leq 2^\circ$. Further, the recent result by HEGRA AIROBICC's 90% CL upper limit (Aharonian et al. 2002) at several tens TeV is also plotted. In subfigure (b), 90% CL upper limit (lower bar) is also shown to compare with the CASA-MIA 90% CL upper limits (Borione et al. 1998) in higher energies, from the OG plane of $50^\circ \leq l \leq 200^\circ$ with $|b| \leq 2^\circ$.

The theoretical curve calculated by Berezhinsky et al. (1993) for $\pi^\circ \rightarrow 2\gamma$ is drawn by a solid curve (BGHS) for the region of $20^\circ \leq l \leq 55^\circ$ and $|b| \leq 2^\circ$. For inverse Compton gamma rays calculated by Porter & Protheroe (1997) is shown by dashed curves for source electron spectral indices of 2.0 (PP2.0) and 2.4 (PP2.4) in the direction $l = 0^\circ$ and $b = 0^\circ$, the Galactic center. Similar theoretical curves calculated by Tateyama & Nishimura (2001) are shown by dot-dashed lines with source spectral indices of 2.0 (TN2.0) and 2.4 (TN2.4) in the direction $l = 0^\circ$ and $|b| \leq 2^\circ$. The present results at 10 TeV give the most stringent upper limit in TeV region for the IC model with a source electron spectral index of 2.0.

This work is supported in part by Grants-in-Aid for Scientific Research on Priority Areas from the Ministry of Education, Culture, Sports, Science and Technology in Japan and from the Committee of the Natural Science Foundation and the Academy of Sciences in China.

1. Aharonian, F.A. et al. 2001, *A&A*, 375, 1008
2. Aharonian, F.A. et al. 2002, *Astropart. phys.*, 17, 459
3. Amenomori, M. et al. 1992, *Phys. Rev. Letters*, 69, 2468
4. ———. 1993, *Phys. Rev. D*, 47, 2675
5. ———. 1996, *ApJ*, 464, 954
6. ———. 2002, *ApJ*, 580, 887
7. Apanasenko, A.V. et al. 2001, *Astropart. Phys.*, 16, 13
8. Berezhinsky, V.S., Gaisser, T.K., Halzen, F., & Stanev, T. 1993, *Astropart. Phys.*, 1, 281
9. Bertsch, D.L. et al. 1993, *ApJ*, 416, 587
10. Borione, A. et al. 1998, *ApJ*, 493, 175
11. Hunter, S.D. et al. 1997, *ApJ*, 481, 205
12. LeBohec, S. et al. 2000, *ApJ*, 539, 209
13. Mori, S. 1997, *ApJ*, 478, 225
14. Pohl, M., & Esposito, J.A. 1998, *ApJ*, 507, 327
15. Porter, T.A., & Protheroe, R.J. 1997, *J. Phys. G*, 23, 1765
16. Tateyama, N., & Nishimura, J. 2001, *Proc. 27th Int. Cosmic Ray Conf. (Hamburg)*, 6, 2343
17. Webber, W.R. 1999, *Proc. 26th Int. Cosmic Ray Conf. (Salt Lake City)*, 4, 97